

Modified Implicit Discretization of the Super-Twisting Controller

Benedikt Andritsch, Lars Watermann, Stefan Koch, Markus Reichhartinger, Johann Reger,
and Martin Horn

Abstract—In this paper a novel discrete-time realization of the super-twisting controller is proposed. The closed-loop system is proven to be globally asymptotically stable in the absence of a disturbance by means of Lyapunov theory. Furthermore, the steady-state error in the disturbed case is computed analytically and shown to be independent of the parameters. The steady-state error only depends on the sampling time and the unknown disturbance. The proposed discrete-time controller is compared to previously published discrete-time super-twisting controllers by means of the controller structure. In extensive simulation studies the proposed controller is evaluated comparative to known controllers. The continuous-time super-twisting controller is capable of rejecting any unknown Lipschitz-continuous perturbation. Furthermore, the convergence time decreases, if any of the gains is increased. The simulations demonstrate that the systems closed in the loop with each of the known controllers lose one of these properties, introduce discretization-chattering effects, or do not yield the same accuracy level as with the proposed controller. The proposed controller, in contrast, is beneficial in terms of the above described properties of the continuous-time super-twisting controller.

Index Terms—Backward Euler discretization, Discrete-time control, Implicit discretization, Sliding mode control, Super-twisting algorithm, Super-twisting control

I. INTRODUCTION

The field of Sliding Mode (SM) Control (SMC) has proven to be of high importance when considering systems with unknown disturbances [1]. In continuous-time, SMC manages to completely reject any disturbances that fulfill some requirements like boundedness or Lipschitz-continuity. However, SM controllers are mostly implemented on discrete-time hardware, requiring appropriate representations of these controllers. Discrete-time SM controllers have to deal with

This work has been submitted to the IEEE for possible publication. Copyright may be transferred without notice, after which this version may no longer be accessible.

The financial support by the Austrian Science Fund (FWF) grant no. I 4152, the Austrian Federal Ministry for Digital and Economic Affairs, the National Foundation for Research, Technology and Development and the Christian Doppler Research Association is gratefully acknowledged. The second and fifth author further acknowledge the financial support by the German Research Foundation (DFG), project no. 416911519, and by the European Union Horizon 2020 research and innovation program under Marie Skłodowska-Curie grant no. 824046.

B. Andritsch and M. Reichhartinger are with the Institute of Automation and Control at Graz University of Technology, Graz, Austria. (email: benedikt.andritsch@tugraz.at, markus.reichhartinger@tugraz.at)

S. Koch and M. Horn are with the Christian Doppler Laboratory for Model-Based Control of Complex Test Bed Systems, Institute of Automation and Control, Graz University of Technology, Graz, Austria. (email: stefan.koch@tugraz.at, martin.horn@tugraz.at)

L. Watermann and Johann Reger are with the Control Engineering Group at Technische Universität Ilmenau, Ilmenau, Germany. (email: lars.watermann@tu-ilmenau.de, johann.reger@tu-ilmenau.de)

unpleasant effects like discretization-chattering, which diminishes the advantageous properties of SMC [2], [3]. One of the first techniques in conventional SMC [1] avoiding discretization-chattering is the implicit discretization [4].

A famous continuous-time SM system is the Super-Twisting Algorithm (STA) [5], [6]. The STA is capable of rejecting Lipschitz-continuous disturbances, which is of high interest in real-world control problems [7], [8]. Therefore, a proper discrete-time implementation of the Super-Twisting Controller (STC) is essential for many applications. The goal of a discrete-time implementation of the STC is to preserve as many properties of the continuous-time controller as possible.

There have been different approaches to achieve an implicitly discretized version of the STC [9], [10]. Also, non-implicit discretization techniques have been applied to the STC, e.g. the matching approach [11]. However, these discrete-time versions fail to resemble some very important properties of the continuous-time STC, like the rejectable class of disturbances, the behavior regarding parameter tuning and the impact of the controller parameters on the steady-state accuracy.

In this paper, an overview of existing discrete-time versions of the STC is given in Section II. Then in Section III a novel implicit discretization of the STC is presented. Further, the closed-loop system is shown to be globally asymptotically stable in the disturbance-free case. The maximum remaining control error in the case of a disturbance is considered analytically. Finally, in extensive simulation studies in Section IV it is demonstrated that the proposed controller preserves all crucial properties of the continuous-time STC, in contrast to previously published controllers.

Mathematical Notations

Let

$$\text{sign}(x) \in \begin{cases} \left\{ \frac{x}{|x|} \right\} & \text{if } x \neq 0 \\ [-1, 1] & \text{if } x = 0 \end{cases}$$

be the signum function with $x \in \mathbb{R}$. Furthermore, the signed power function

$$[x]^y = \text{sign}(x) |x|^y,$$

with $x, y \in \mathbb{R}$ will be used. Note that $[x]^0 = \text{sign}(x)$. Furthermore, let

$$\text{sat}(x) = \begin{cases} x & \text{if } |x| < 1 \\ \text{sign}(x) & \text{else} \end{cases}$$

be the saturation function.

II. RELATED WORK

The STC considers the continuous-time plant

$$\begin{aligned}\dot{x}_1 &= u + \varphi, \\ \dot{\varphi} &= \Delta,\end{aligned}\quad (1)$$

with the state variables x_1 and φ , the control variable u and the unknown disturbance $\Delta(t)$ with $|\Delta| < L$ for some constant L . Thus, φ is Lipschitz-continuous.

The SM-based dynamic state controller

$$\begin{aligned}u &= -\alpha[x_1]^{\frac{1}{2}} + \nu, \\ \dot{\nu} &= -\beta[x_1]^0,\end{aligned}\quad (2)$$

with the controller state ν is known as STC and stabilizes $x_1 = 0$ of (1) if the constant gains α and β are chosen accordingly [5]. The closed-loop system

$$\begin{aligned}\dot{x}_1 &= -\alpha[x_1]^{\frac{1}{2}} + x_2, \\ \dot{x}_2 &= -\beta[x_1]^0 + \Delta,\end{aligned}\quad (3)$$

with $x_2 = \varphi + \Delta$ resulting from the plant (1) and the STC (2) is called STA.

The goal of implementing the STC is to determine a discrete-time representation of the controller (2), which can generally be written as

$$\begin{aligned}u_k &= -\alpha\Psi_1(x_{1,k}) + \nu_{k+1}, \\ \nu_{k+1} &= \nu_k - h\beta\Psi_2(x_{1,k}),\end{aligned}\quad (4)$$

with the state dependent functions Ψ_1 and Ψ_2 , the discretization-time h , the known discrete-time system state $x_{1,k} = x_1(kh)$, and $k = 1, 2, \dots$. The discrete-time control variable u_k is then fed to the continuous-time system through a zero-order hold element, i.e. $u(t) = u_k$ for $kh \leq t < (k+1)h$. Note that u_k contains the controller-state at $k+1$, i.e. ν_{k+1} , as in this paper mainly implicit discretization approaches are considered. Denote by C_* the controller resulting from (4) and specific controller functions $\Psi_{1,*}$ and $\Psi_{2,*}$. In the following, several discrete-time realizations of the STC are presented.

A. Implicit Discretization

One discrete-time STC was published in [9], [12] by Brogliato *et al.* and can be written as

$$\begin{aligned}\Psi_{1,\text{Brogliato}} &= -\text{sign}(x_{1,k}) \left(-\frac{h\alpha}{2} + \sqrt{\frac{h^2\alpha^2}{4} + \max(0, |x_{1,k} + hv_k| - h^2\beta)} \right), \\ \Psi_{2,\text{Brogliato}} &= \text{sat}\left(\frac{x_{1,k} + hv_k}{h^2\beta}\right).\end{aligned}\quad (5)$$

Note that $\Psi_{1,\text{Brogliato}}$ depends not only on the plant state $x_{1,k}$, but also on the controller state ν_k . The authors use an implicit discretization approach to establish the explicitly given discrete-time controller functions (5). It is proven that the undisturbed closed-loop system is globally asymptotically stable. However, the authors also describe that the plant state

x_1 is affected by the perturbation proportional to h . The authors introduce the sliding variable $x_{1,k} + hv_k$, which is driven to zero and maintained there. Also, $C_{\text{Brogliato}}$ drives the closed-loop state $\varphi_k + \nu_k$ to zero.

However, let us assume an unbounded perturbation φ_k , e.g. due to a constant disturbance Δ_k . Then φ_k will grow, and thus, also ν_k will grow. With the sliding variable kept at the origin, therefore also $x_{1,k}$ will grow and the control goal $x_{1,k} = 0$ can not be maintained. Therefore, the controller $C_{\text{Brogliato}}$ is not able to reject an unbounded perturbation φ , which reduces the class of disturbances Δ that can be handled by the controller compared to the continuous-time STC. These thoughts will be discussed in simulations in Section IV as well.

B. Discretization Based on Matching Approach

Another discrete-time implementation of the controller (2) is presented in [11], [13] by Koch *et al.* The authors utilize the matching approach to establish a discrete-time controller, resulting in the controller functions

$$\begin{aligned}\Psi_{1,\text{Koch}} &= -\frac{1}{\alpha h} \left(e^{\frac{p_1 h}{\sqrt{|x_{1,k}|}}} + e^{\frac{p_2 h}{\sqrt{|x_{1,k}|}}} - 2 \right) x_{1,k} - \frac{h\beta}{\alpha} \Psi_{2,\text{Koch}}, \\ \Psi_{2,\text{Koch}} &= \frac{1}{h^2\beta} \left(e^{\frac{p_1 h}{\sqrt{|x_{1,k}|}}} - 1 \right) \left(e^{\frac{p_2 h}{\sqrt{|x_{1,k}|}}} - 1 \right) x_{1,k},\end{aligned}\quad (6)$$

with $p_{1,2} = -\frac{\alpha}{2} \pm \sqrt{\frac{\alpha^2}{4} - \beta}$. The discrete-time closed-loop system is shown to avoid discretization-chattering effects and to be globally asymptotically stable in the disturbance-free case. Note that $\Psi_{1,\text{Koch}}$ differs from the function in [11] due to the different definition of the general discrete-time controller (4).

C. Semi-Implicit Discretization

The third known discrete-time version of the STC that is considered in this paper was published in [10] by Xiong *et al.* and is obtained by a semi-implicit discretization. It consists of the controller functions

$$\begin{aligned}\Psi_{1,\text{Xiong}} &= \frac{1}{h\alpha} D_k \text{sat}\left(\frac{x_{1,k}}{D_k}\right), \\ \Psi_{2,\text{Xiong}} &= \text{sat}\left(\frac{x_{1,k}}{D_k}\right),\end{aligned}\quad (7)$$

where

$$D_k = \begin{cases} h\alpha|x_{1,k}|^{\frac{1}{2}} + h^2\beta & \text{if } |x_{1,k}| > h\alpha|x_{1,k}|^{\frac{1}{2}} + h^2\beta \\ h^2\beta & \text{else.} \end{cases}$$

The authors show that the controller is insensitive to an overestimation of the gains regarding the asymptotic accuracy of the closed-loop system.

D. Low-Chattering Discretization

Finally, the last considered discrete-time STC is derived from the low-chattering differentiator presented in [14]. The controller functions take the form

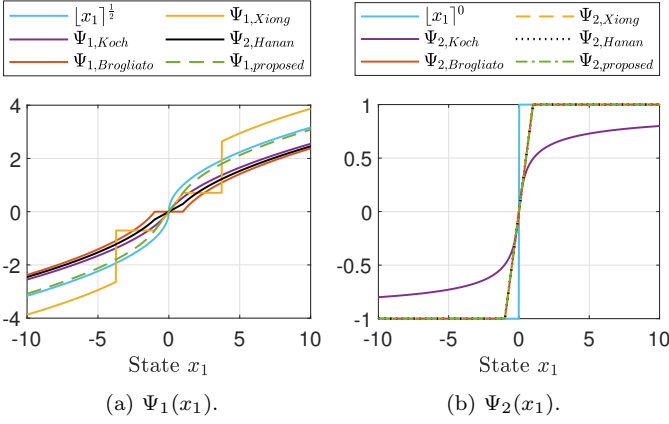


Fig. 1: Compared controller functions.

$$\begin{aligned}\Psi_{1,Hanan} &= \text{sat}\left(\frac{|x_{1,k}|}{\beta h^2}\right)^{\frac{1}{2}} [x_{1,k}]^{\frac{1}{2}} - \frac{h\beta}{\alpha} \text{sat}\left(\frac{x_{1,k}}{\beta h^2}\right), \\ \Psi_{2,Hanan} &= \text{sat}\left(\frac{x_{1,k}}{\beta h^2}\right).\end{aligned}\quad (8)$$

A detailed derivation of this discrete-time representation of the STC is given in Appendix B.

Fig. 1a and 1b show the discrete-time controller functions $\Psi_{1,j}(x_1)$ respective $\Psi_{2,j}(x_1)$ with $j \in \{\text{Brogliato, Koch, Xiong, Hanan}\}$ from (5), (6), (7) and (8), as well as the functions $|x_1|^{\frac{1}{2}}$ respective $|x_1|^0$ from the continuous-time controller (2). The parameters were chosen as $h = 1$, $\beta = 1$, $\alpha = \sqrt{2\beta}$. For the computation of $\Psi_{1,Brogliato}(x_1)$ and $\Psi_{2,Brogliato}(x_1)$, v_k was assumed to be zero. This is the case in steady state in the absence of a disturbance. Fig. 1a shows two regions within x_1 , where $\Psi_{1,Xiong}$ is constant. Between these regions, $\Psi_{1,Xiong}$ is linear. The size of the constant regions depends on the parameters α and β and is large w.r.t. the linear region, when α is large compared to β . The effect of this linear region will be discussed in Section IV.

III. PROPOSED DISCRETE-TIME STC

Sampling the continuous-time state $x_1(t)$ of system (1) with $u(t) = u_k \forall t \in [kh, (k+1)h)$ results in

$$x_1((k+1)h) = x_1(kh) + hu_k + \int_{kh}^{(k+1)h} \varphi(\tau) d\tau.$$

From this the discrete-time plant model

$$\begin{aligned}x_{1,k+1} &= x_{1,k} + hu_k + h\varphi_k, \\ \varphi_{k+1} &= \varphi_k + h\Delta_k\end{aligned}\quad (9)$$

is derived, with the discrete-time unknown input Δ_k fulfilling $|\Delta_k| \leq L$, which is used in the following considerations. Note that, eventhough (9) is structurally equivalent to an Euler explicit discretization of the plant (1), the state $x_{1,k}$ coincides with the exact samples $x_1(kh)$. For details on the derivation see Appendix A.

The novel discrete-time STC functions

$$\begin{aligned}\Psi_{1,proposed} &= \text{sign}(x_{1,k}) \left(\frac{h\beta}{\alpha} \text{sat}\left(\frac{|x_{1,k}|}{h^2\beta}\right) - \frac{h\alpha}{2} + \sqrt{\frac{h^2\alpha^2}{4} + \max(0, |x_{1,k}| - h^2\beta)} \right), \\ \Psi_{2,proposed} &= \text{sat}\left(\frac{x_{1,k}}{h^2\beta}\right)\end{aligned}\quad (10)$$

are proposed in this paper for the discrete-time plant model (9). Note that the controller functions (10) resemble the terms of the implicit controller functions (5), with $x_{1,k} + hv_k$ replaced by $x_{1,k}$, and extended by the saturation term in the equation for $\Psi_{1,proposed}$. The controller can therefore be regarded as a modified implicitly discretized STC.

Fig. 1a and 1b also show the functions $\Psi_{1,proposed}$ and $\Psi_{2,proposed}$, respectively. Note that $\Psi_{2,proposed}$, $\Psi_{2,Brogliato}$, $\Psi_{2,Xiong}$ and $\Psi_{2,Hanan}$ coincide. Furthermore, $\Psi_{1,proposed}$ and $\Psi_{1,Xiong}$ coincide near the origin, i.e. at $|x_1| \leq h^2\beta$.

Let the unknown virtual state $x_{2,k}$ be defined as $x_{2,k} := v_k + \varphi_k$. The closed-loop system resulting from the discrete-time plant (9) and the controller $\mathcal{C}_{proposed}$ is

$$\begin{aligned}x_{1,k+1} &= x_{1,k} - 2h^2\beta \text{sat}\left(\frac{x_{1,k}}{h^2\beta}\right) - h\alpha \text{sign}(x_{1,k}) \left(-\frac{h\alpha}{2} + \sqrt{\frac{h^2\alpha^2}{4} + \max(0, |x_{1,k}| - h^2\beta)} \right) + hx_{2,k}, \\ x_{2,k+1} &= x_{2,k} - h\beta \text{sat}\left(\frac{x_{1,k}}{h^2\beta}\right) + h\Delta_k.\end{aligned}\quad (11)$$

In the following, the stability properties of the discrete-time STA (11) are examined.

Theorem 3.1: In the absence of a disturbance, i.e. $\Delta_k \equiv 0$, the origin of the closed-loop system (11) is globally asymptotically stable.

Proof 3.2: In order to attend the stability properties of the closed-loop system, Lyapunov theory is applied. In this proof, only the undisturbed plant, i.e. $\Delta_k \equiv 0$, is considered. Inspired by the stability analysis in [11, Theorem IV.1] define the Lyapunov candidate $V_k = \mu|x_{1,k} - hx_{2,k}| + x_{2,k}^2$, $\mu \in \mathbb{R}^+$. In general, using (4) the next step of the Lyapunov candidate computes to

$$\begin{aligned}V_{k+1} &= \mu|x_{1,k+1} - hx_{2,k+1}| + x_{2,k+1}^2 \\ &= \mu|x_{1,k} - h\alpha\Psi_1(x_{1,k})| + (x_{2,k} - h\beta\Psi_2(x_{1,k}))^2.\end{aligned}$$

For the proposed controller, this yields

$$\begin{aligned}V_{k+1} &= \mu \left| x_{1,k} - h^2\beta \text{sat}\left(\frac{x_{1,k}}{h^2\beta}\right) - h\alpha \text{sign}(x_{1,k}) \cdot \left(-\frac{h\alpha}{2} + \sqrt{\frac{h^2\alpha^2}{4} + \max(0, |x_{1,k}| - h^2\beta)} \right) \right| + \\ &\quad + \left(x_{2,k} - h\beta \text{sat}\left(\frac{x_{1,k}}{h^2\beta}\right) \right)^2.\end{aligned}$$

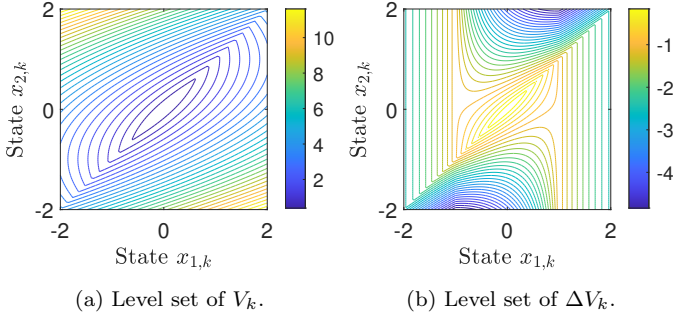


Fig. 2: Level sets of the Lyapunov candidate V_k and its difference ΔV_k .

Fig. 2 shows the level sets of the functions V_k and $\Delta V_k = V_{k+1} - V_k$.

Case 1: $|x_{1,k}| \leq h^2\beta$ gives

$$V_{k+1} = \mu \left| x_{1,k} - x_{1,k} - h\alpha \text{sign}(x_{1,k}) \left(-\frac{h\alpha}{2} + \sqrt{\frac{h^2\alpha^2}{4}} \right) \right| + \left(x_{2,k} - \frac{1}{h}x_{1,k} \right)^2 = \left(x_{2,k} - \frac{1}{h}x_{1,k} \right)^2.$$

The difference $\Delta V_k = V_{k+1} - V_k$ then computes to

$$\begin{aligned} \Delta V_k &= -\mu |x_{1,k} - hx_{2,k}| + \left(x_{2,k} - \frac{1}{h}x_{1,k} \right)^2 - x_{2,k}^2 = \\ &= -\mu |x_{1,k} - hx_{2,k}| + \frac{x_{1,k}^2}{h^2} (x_{1,k} - hx_{2,k}) - \frac{x_{1,k}x_{2,k}}{h}. \end{aligned}$$

It is evident that $\Delta V_k = 0$ for $x_{1,k} = x_{2,k} = 0$. All other state values are distinguished in two cases with the upper limit

$$\begin{aligned} \Delta V_k &\leq \left(\frac{|x_{1,k}|}{h^2} - \mu \right) |x_{1,k} - hx_{2,k}| - \frac{x_{1,k}x_{2,k}}{h} \\ &\leq (\beta - \mu) |x_{1,k} - hx_{2,k}| - \frac{x_{1,k}x_{2,k}}{h}, \end{aligned}$$

established with $|x_{1,k}| \leq h^2\beta$.

Case 1.a: $\text{sign}(x_{1,k}) = \text{sign}(x_{2,k})$ or $x_{1,k} = 0, x_{2,k} \neq 0$ or $x_{1,k} \neq 0, x_{2,k} = 0$ yields

$$\Delta V_k \leq \underbrace{(\beta - \mu)}_{<0} \underbrace{|x_{1,k} - hx_{2,k}|}_{\geq 0} - \underbrace{\frac{|x_{1,k}x_{2,k}|}{h}}_{\geq 0},$$

where not both non-negative terms can be zero at the same time. By choosing $\mu > \beta$, e.g. $\mu = 2\beta$, ΔV_k is hence assured to be negative.

Case 1.b: $\text{sign}(x_{1,k}) \neq \text{sign}(x_{2,k}), x_{1,k} \neq 0, x_{2,k} \neq 0$ gives

$$|x_{1,k} - hx_{2,k}| > |hx_{2,k}|$$

Thus, with the selection $\mu = 2\beta$ and $|x_{1,k}| \leq h^2\beta$

$$\begin{aligned} \Delta V_k &\leq -\beta |x_{1,k} - hx_{2,k}| + \frac{|x_{1,k}x_{2,k}|}{h} \\ &< -h\beta |x_{2,k}| + \frac{|x_{1,k}x_{2,k}|}{h} \\ &\leq -h\beta |x_{2,k}| + h\beta |x_{2,k}| = 0 \\ \Rightarrow \Delta V_k &< 0 \end{aligned}$$

holds.

Case 2: $|x_{1,k}| > h^2\beta$ yields

$$V_{k+1} = \mu \left| x_{1,k} - \text{sign}(x_{1,k}) \left(h^2\beta + h\alpha \left(-\frac{h\alpha}{2} + \sqrt{\frac{h^2\alpha^2}{4} + |x_{1,k}| - h^2\beta} \right) \right) \right| + (x_{2,k} - \text{sign}(x_{1,k})h\beta)^2.$$

Let us introduce $z_{1,k} := x_{1,k} - \text{sign}(x_{1,k})h^2\beta$, $z_{2,k} := x_{2,k} - \text{sign}(x_{1,k})h\beta$, with $z_{1,k} \in \mathbb{R} \setminus \{0\}$ and $z_{2,k} \in \mathbb{R}$. Note that $\text{sign}(x_{1,k}) = \text{sign}(z_{1,k})$. This gives

$$\begin{aligned} V_k &= \mu |z_{1,k} - hz_{2,k}| + z_{2,k}^2 + \text{sign}(z_{1,k})2h\beta z_{2,k} + h^2\beta^2, \\ V_{k+1} &= \mu \left| z_{1,k} - h\alpha \text{sign}(z_{1,k}) \left(-\frac{h\alpha}{2} + \sqrt{\frac{h^2\alpha^2}{4} + |z_{1,k}|} \right) \right| + z_{2,k}^2, \end{aligned}$$

and further

$$\begin{aligned} \Delta V_k &= \mu \left(\left| z_{1,k} - h\alpha \text{sign}(z_{1,k}) \left(-\frac{h\alpha}{2} + \sqrt{\frac{h^2\alpha^2}{4} + |z_{1,k}|} \right) \right| - \right. \\ &\quad \left. |z_{1,k} - hz_{2,k}| \right) - 2h\beta \text{sign}(z_{1,k})z_{2,k} - h^2\beta^2. \end{aligned}$$

Note that ΔV_k is an odd function with respect to the origin, as

$$\begin{aligned} \Delta V_k &= \mu \left(\left| z_{1,k} - h\alpha \text{sign}(z_{1,k}) \left(-\frac{h\alpha}{2} + \sqrt{\frac{h^2\alpha^2}{4} + |z_{1,k}|} \right) \right| - \right. \\ &\quad \left. |z_{1,k} - hz_{2,k}| \right) - 2h\beta \text{sign}(z_{1,k})z_{2,k} - h^2\beta^2 \\ &= \mu \left(\left| -z_{1,k} - h\alpha \text{sign}(-z_{1,k}) \left(-\frac{h\alpha}{2} + \sqrt{\frac{h^2\alpha^2}{4} + |-z_{1,k}|} \right) \right| - \right. \\ &\quad \left. |-z_{1,k} + hz_{2,k}| \right) - 2h\beta \text{sign}(-z_{1,k})(-z_{2,k}) - h^2\beta^2. \end{aligned}$$

Therefore, it is sufficient to only consider the case $z_{1,k} > 0$, which yields

$$\begin{aligned} \Delta V_k &= \mu \left(\underbrace{\left| z_{1,k} - h\alpha \left(-\frac{h\alpha}{2} + \sqrt{\frac{h^2\alpha^2}{4} + z_{1,k}} \right) \right|}_{(=:A)} - |z_{1,k} - hz_{2,k}| \right) - \\ &\quad - 2h\beta z_{2,k} - h^2\beta^2, \end{aligned} \quad (12)$$

and is assumed in the remaining part of the proof. Note that also $A > 0$ holds.

The objective is to show that $\Delta V_k < 0$ holds for all states $(z_{1,k}, z_{2,k})$. This is done by distinguishing several cases. In all cases the selection $\mu = 2\beta$ is used.

Case 2.a: $z_{1,k} - A \geq 0$ and $z_{1,k} - hz_{2,k} \geq 0$ leads to

$$\begin{aligned} \Delta V_k &= \mu(hz_{2,k} - A) - 2h\beta z_{2,k} - h^2\beta^2 \\ &\stackrel{\mu=2\beta}{=} -2\beta A - h^2\beta^2 < 0. \end{aligned}$$

Case 2.b: $z_{1,k} - A \geq 0$ and $z_{1,k} - hz_{2,k} < 0$ gives

$$\begin{aligned} \Delta V_k &= \mu(2z_{1,k} - A - hz_{2,k}) - 2h\beta z_{2,k} - h^2\beta^2 \\ &\stackrel{\mu=2\beta}{=} 4\beta \underbrace{(z_{1,k} - hz_{2,k})}_{<0} - 2\beta A - h^2\beta^2 < 0. \end{aligned}$$

Case 2.c: $z_{1,k} - A < 0$ and $z_{1,k} - hz_{2,k} \geq 0$ yields

$$\begin{aligned} \Delta V_k &= \mu(A - 2z_{1,k} + hz_{2,k}) - 2h\beta z_{2,k} - h^2\beta^2 \\ &\stackrel{\mu=2\beta}{=} 2\beta(A - 2z_{1,k}) - h^2\beta^2. \end{aligned} \quad (13)$$

Inserting A from (12) into (13) gives the inequality to be shown

$$\begin{aligned} 2\beta h\alpha \left(-\frac{h\alpha}{2} + \sqrt{\frac{h^2\alpha^2}{4} + z_{1,k}} \right) - 4\beta z_{1,k} - h^2\beta^2 &< 0 \\ \Leftrightarrow \sqrt{\frac{h^2\alpha^2}{4} + z_{1,k}} &< \frac{h\beta}{2\alpha} + \frac{2z_{1,k}}{h\alpha} + \frac{h\alpha}{2} \\ \Leftrightarrow \frac{h^2\alpha^2}{4} + z_{1,k} &< \frac{h^2\beta^2}{4\alpha^2} + \frac{4z_{1,k}^2}{h^2\alpha^2} + \frac{h^2\alpha^2}{4} + \frac{2\beta z_{1,k}}{\alpha^2} + \frac{h^2\beta}{2} + 2z_{1,k} \\ \Leftrightarrow 0 &< \underbrace{z_{1,k}^2}_{>0} \underbrace{\frac{4}{h^2\alpha^2}}_{>0} + \underbrace{z_{1,k}}_{>0} \underbrace{\left(\frac{2\beta}{\alpha^2} + 1 \right)}_{>0} + \underbrace{\left(\frac{h^2\beta^2}{4\alpha^2} + \frac{h^2\beta}{2} \right)}_{>0}. \end{aligned}$$

The inequality in the last line holds and thus $\Delta V_k < 0$.

Case 2.d: $z_{1,k} - A < 0$ and $z_{1,k} - hz_{2,k} < 0$ leads to

$$\begin{aligned} \Delta V_k &= \mu(A - hz_{2,k}) - 2h\beta z_{2,k} - h^2\beta^2 \\ &\stackrel{\mu=2\beta}{=} 2\beta(A - 2hz_{2,k}) - h^2\beta^2. \end{aligned}$$

Using the lower bound $z_{1,k} < hz_{2,k}$ for $hz_{2,k}$ yields

$$\Delta V_k < 2\beta(A - 2z_{1,k}) - h^2\beta^2 < 0,$$

where the last inequality was already shown in Case 2.c.

In the cases above all possible combinations of states $(x_{1,k}, x_{2,k})$ were considered. In all cases $(x_{1,k}, x_{2,k}) \neq (0, 0)$, $\Delta V_k(x_{1,k}, x_{2,k}) < 0$ was proven with $\Delta V_k(0, 0) = 0$. Therefore, V_k with $\mu = 2\beta$ is a discrete-time Lyapunov function for the closed-loop system (11) and thus, the origin of the system is globally asymptotically stable in the undisturbed case.

Theorem 3.3: Consider the closed-loop system (11) with the Lipschitz constant L , i.e. $|\Delta_k| \leq L \forall k$. If $|x_{1,k}| \leq h^2\beta$ and $|hx_{2,k} - x_{1,k}| \leq h^2\beta$ is fulfilled for some $k = K$, the steady-state error $\limsup_{k \geq K} |x_{1,k}| \leq e_{\max}$ is limited by $e_{\max} = h^2L$. Further, the closed-loop system is exact in the absence of a disturbance, i.e. the state $x_{1,k}$ converges to zero. Thus, discretization-chattering is completely avoided.

Proof 3.4: Assume $|x_{1,k}| \leq h^2\beta$. Then (10) can be simplified to

$$\begin{aligned} u_k &= -\frac{2}{h}x_{1,k} + v_k, \\ v_{k+1} &= v_k - \frac{1}{h}x_{1,k}. \end{aligned} \quad (14)$$

The second-order closed-loop system resulting from (9) and (14) is then given by

$$\begin{aligned} x_{1,k+1} &= -x_{1,k} + hx_{2,k}, \\ x_{2,k+1} &= x_{2,k} - \frac{1}{h}x_{1,k} + h\Delta_k, \end{aligned}$$

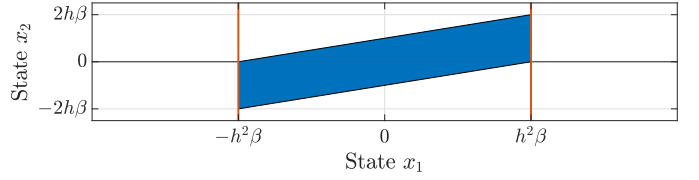


Fig. 3: Forward invariant set \mathcal{M} of the closed-loop system.

or in matrix-form

$$\begin{bmatrix} x_{1,k+1} \\ x_{2,k+1} \end{bmatrix} = \underbrace{\begin{bmatrix} -1 & h \\ -\frac{1}{h} & 1 \end{bmatrix}}_A \begin{bmatrix} x_{1,k} \\ x_{2,k} \end{bmatrix} + \begin{bmatrix} 0 \\ h \end{bmatrix} \Delta_k. \quad (15)$$

The eigenvalues of the system-matrix A are both zero, which means that (15) is a second-order dead-beat system [15]. Thus, the steady state is reached after two steps. In steady state the unknown input Δ_k affects the system state $x_{1,k}$ proportional to h^2 .

The discrete-time controller acts as a dead-beat controller, whenever $|x_{1,k}| \leq h^2\beta$. In order to reach steady state, the dead-beat controller (14) must be applied to the plant two times consecutively. Thus, to reach steady state $|x_{1,k}| \leq h^2\beta$ and $|x_{1,k+1}| \leq h^2\beta$ must hold. According to (15) this means

$$|x_{1,k+1}| \leq h^2\beta \Leftrightarrow |hx_{2,k} - x_{1,k}| \leq h^2\beta,$$

which results in the forward invariant set $\mathcal{M} = \{(x_{1,k}, x_{2,k}) \in \mathbb{R}^2 \mid |x_{1,k}| \leq h^2\beta, |hx_{2,k} - x_{1,k}| \leq h^2\beta\}$ of the closed-loop system (11). The set \mathcal{M} is plotted in Fig. 3 in state-space as a blue area. Everywhere between the red lines the dead-beat controller is applied to the system. Due to Theorem 3.1 this region is reached for sure if $\Delta_k \equiv 0$.

IV. EVALUATION IN SIMULATION STUDIES

In this section, the results of numerical simulations are presented. The results of the controller $\mathcal{C}_{\text{proposed}}$ is depicted in green and is compared to the results of the controllers known from literature: $\mathcal{C}_{\text{Brogliato}}$ presented in red, $\mathcal{C}_{\text{Koch}}$ shown in purple, $\mathcal{C}_{\text{Xiong}}$ outlined in orange, $\mathcal{C}_{\text{Hanan}}$ depicted in black, and the Euler explicit discretization $\mathcal{C}_{\text{explicit}}$ of (2) drawn as blue lines. All simulations were performed in MATLAB[®]/Simulink[®]. In the following, Σ_* denotes the simulated closed-loop system consisting of the simulated continuous-time plant and the discrete-time controller \mathcal{C}_* . It is shown in what regard $\mathcal{C}_{\text{proposed}}$ is an improvement to state-of-the-art discrete-time STCs.

A. Simulations with Disturbance in Time-Domain

The first simulation was performed with a constant disturbance $\Delta = 1 \forall t \geq 1$ and $\Delta = 0 \forall t < 1$. The parameters were chosen as $\alpha = \sqrt{10}$, $\beta = 10$, $h = 0.01$ and $x_1(0) = 1$. The second simulation was performed with the same parameters and a disturbance known from literature [10], [13] with a constant offset of 5, $\Delta(t) = 1.2 \cos(2t) + 0.4\sqrt{10} \cos(\sqrt{10}t) + 5$. The results are presented in Fig. 4a and 4b, where the disturbance Δ is outlined in light blue and scaled by 0.05. The results clearly show that the $\mathcal{C}_{\text{Brogliato}}$ is not capable of rejecting constant parts of the disturbance Δ , as it was described in Section II. All other controllers result in a state x_1 converging close to zero.

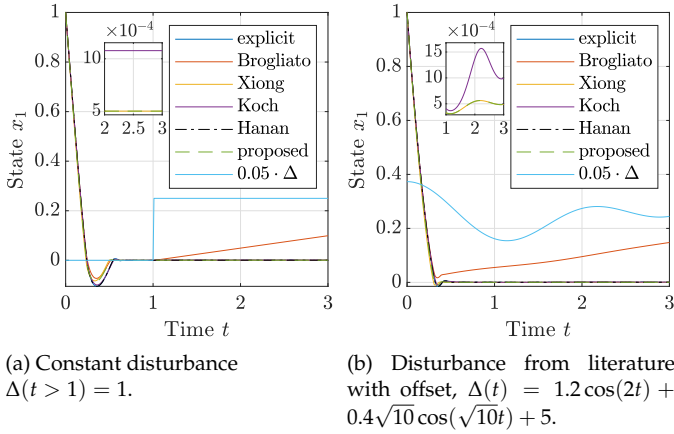


Fig. 4: Simulation of the compared systems in time-domain with a disturbance, $\alpha = \sqrt{10}$, $\beta = 10$, $h = 0.01$ and $x_1(0) = 1$.

B. Simulations without Disturbance in Time-Domain

Three more simulations were performed with no disturbance, i.e. $\Delta \equiv 0$. In Fig. 5a $\alpha = \sqrt{10}$ was chosen as before. In Fig. 5b the parameter was set to $\alpha = 30$, which is large w.r.t. β , and in Fig. 5c $\alpha = 1.5\sqrt{\beta/1.1}$ was set according to the recommended parameter choice for $\mathcal{C}_{\text{Hanan}}$ in [14, Fig. 3]. The other parameters remained unchanged, i.e. $\beta = 10$, $h = 0.01$ and $x_1(0) = 1$. The state x_1 is depicted in absolute values and scaled logarithmically in these plots, in order to emphasize the differences between the results of the controllers. The results show that Σ_{explicit} is not exact and shows discretization-chattering in steady state. In Fig. 5c all other systems converge to zero without discretization-chattering effects, however, Σ_{Hanan} converges slower than the other systems. In Fig. 5a and 5b also Σ_{Hanan} shows discretization-chattering similar to Σ_{explicit} in steady state. In Fig. 5a it can be observed that Σ_{Koch} converges slightly slower to zero compared to Σ_{proposed} . The system $\Sigma_{\text{Brogliato}}$ converges similarly fast as Σ_{proposed} , and Σ_{Xiong} does so slightly faster. From the continuous-time STA (3) it is expected that increasing the parameter α leads to faster convergence times. However, increasing α from $\sqrt{10}$ to 30 in Fig. 5b shows an increased convergence time of Σ_{Xiong} . The systems Σ_{proposed} and $\Sigma_{\text{Brogliato}}$ converge faster to zero.

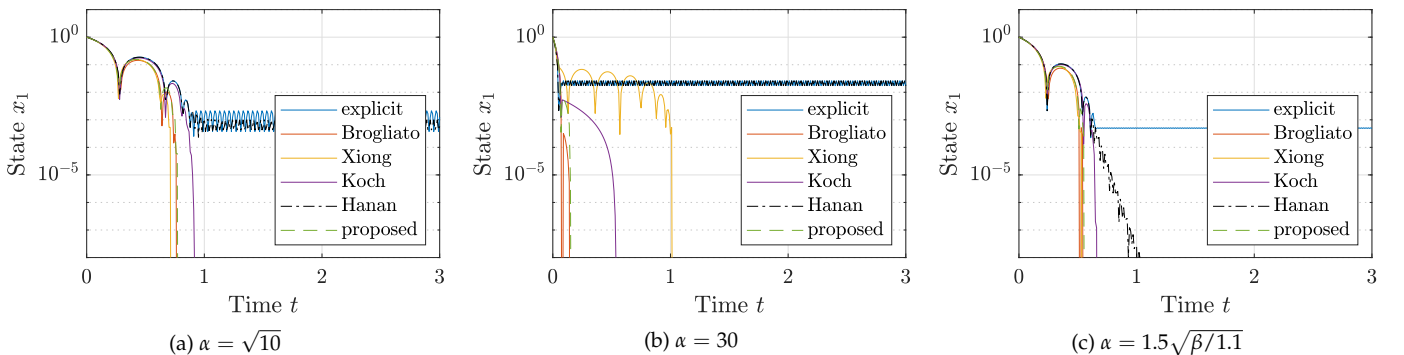


Fig. 5: Simulation of the compared systems in time-domain in the undisturbed case, $\beta = 10$, $h = 0.01$ and $x_1(0) = 1$.

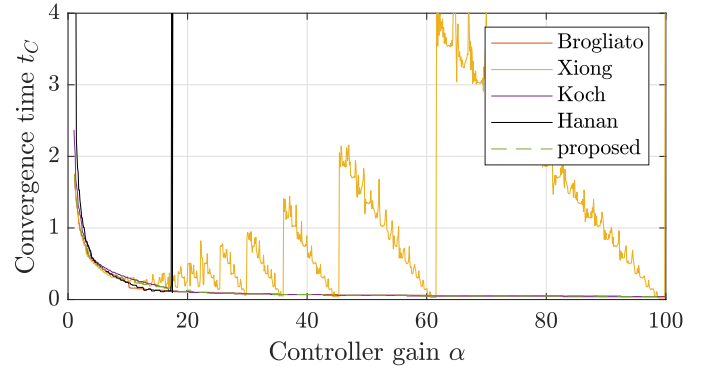


Fig. 6: Convergence time t_C over varying parameter α .

System Σ_{Koch} exhibits a larger convergence time than Σ_{proposed} and $\Sigma_{\text{Brogliato}}$.

C. Convergence Time when Varying One Controller Parameter

In order to analyze the behavior of increasing convergence times when increasing α , the convergence time was determined for several parameter values α . Let the convergence time t_C be defined as follows: A system is said to have reached steady state, i.e. be converged, as soon as the absolute state value does not exceed 1% of the initial value, i.e. $|x_1(t)| \leq 10^{-2}|x_1(0)| \forall t \geq t_C$. Fig. 6 shows the convergence times of the compared systems over the parameter α , which was set to values between 1 and 100, i.e. 0.1β and 10β , in intervals of 0.1. The other parameters were fixed at $\beta = 10$, $h = 0.01$ and $x_1(0) = 1$. It can be observed that the convergence time of Σ_{Hanan} decreases up to some $\alpha \approx 17$, when it increases out of scope of the figure. This again shows that $\mathcal{C}_{\text{Hanan}}$ requires some relation between the two controller parameters α and β and results in discretization-chattering when this relation is not met, as previously seen in Fig. 5. Further, Fig. 6 illustrates that the convergence time of Σ_{Xiong} behaves very sensitive to changes in α when $\alpha > \beta$. Small changes in α can lead to a large increase of the convergence time, e.g. changing α from 29.8 to 29.9 results in t_C changing from 0.11 to 0.87 (all numbers are rounded). The reason for the large convergence times of Σ_{Xiong} when $\alpha > \beta$ may be connected to the constant regions of the controller function $\Psi_{1, \text{Xiong}}$ in (7) which is depicted in Fig. 1a. When α is large

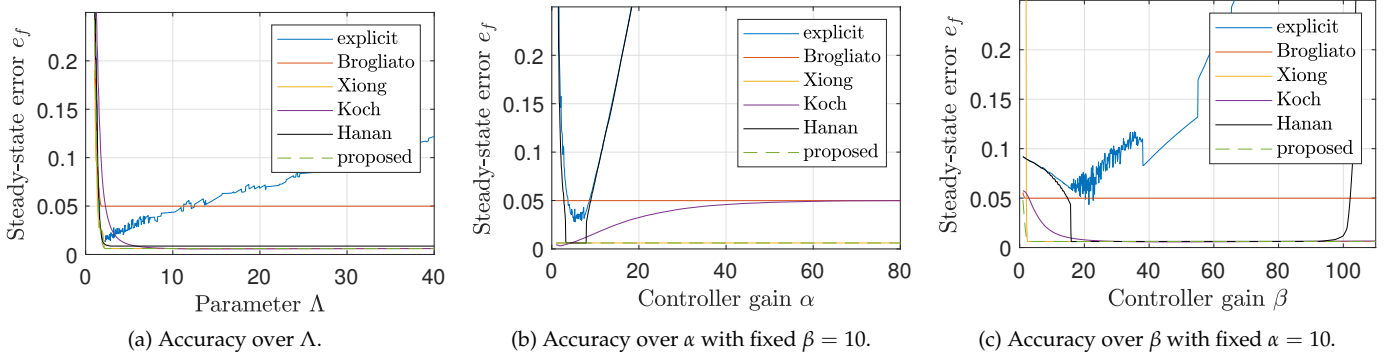


Fig. 7: Accuracy by means of the steady-state error e_f , $h = 0.05$ and $x_1(0) = 0$.

w.r.t. β , then the constant regions are larger w.r.t. the linear region of $\Psi_{1, Xiong}$, as described in Section II. The function $\Psi_{1, Xiong}$ can be interpreted as a rate at which x_1 approaches the origin. When this function is constant with a rather small magnitude, this approaching phase could then take longer, the larger this constant region is.

D. Steady-State Accuracy when Varying the Controller Parameters

Finally, simulations were performed regarding the accuracy of the closed-loop systems, i.e. the remaining steady-state error. Let this steady-state error be defined as $e_f = \limsup_t |x_1|$, with the initial value $x_1(0) = 0$. The systems were simulated until $t = 20$. The disturbance was chosen as $\Delta(t) = 1.2 \cos(2t) + 0.4\sqrt{10} \cos(\sqrt{10}t)$, which was also used in [10], [13]. The discretization time was set to $h = 0.05$. Fig. 7a depicts e_f over the value Λ , which determines the parameters $\alpha = 1.5\sqrt{\Lambda}$ and $\beta = 1.1\Lambda$. This parameter relation corresponds to the suggested parameter choice in [14] and was also applied in [10], where the same simulation was performed. The value Λ was varied between 1 and 40 in 1000 steps. The results from [10] were reproduced, whereas Σ_{proposed} and Σ_{Hanan} performed very similar to Σ_{Xiong} . Fig. 7b and 7c show e_f over varying α and β from 1 to 80 and 110, respectively, in 1000 steps. The second controller parameter was fixed at 10. The results again show the exactness of Σ_{proposed} as well as Σ_{Xiong} , which yield the same small steady-state error after some minimal gain values. The system $\Sigma_{\text{Brogliato}}$, however, settles at larger errors, due to the appearance of the attenuated perturbation φ in x_1 in steady state. In the results of Σ_{Koch} , which is not the result of an implicit approach, a dependency between the controller parameters α and β and the steady-state error can be observed. Increasing α even drives the steady-state error of Σ_{Koch} to the same level where $\Sigma_{\text{Brogliato}}$ settles, as can be seen in Fig. 7b. The system Σ_{Hanan} achieves small steady-state errors within some bounds of α and β , respectively. Outside of these bounds, the accuracy of Σ_{Hanan} approaches the accuracy of Σ_{explicit} , which once again indicates the need of a relation between the parameters.

V. CONCLUSION

In this paper, a novel discrete-time super-twisting controller is presented. It is shown to yield a globally asymptotically

stable closed-loop system in the undisturbed case by means of Lyapunov theory. Furthermore, the steady-state error is proven to not depend on any controller parameters but only on the discretization time and the disturbance. Additionally, the absence of any discretization-chattering effects is shown. The controller is directly compared to previously published discrete-time super-twisting controllers analytically regarding the controller structure as well as in simulation studies. The simulations showed that the presented controller resembles best the properties of the continuous-time controller. The proposed discretization introduces no discretization-chattering effects. Moreover, it can handle all Lipschitz-continuous perturbations. Further, the presented controller yields a steady-state error that is independent of the controller gains. Finally, its convergence time decreases when any of the controller gains is increased. These are all crucial properties of the continuous-time super-twisting controller. The proposed discrete-time super-twisting controller unites all of these properties, in contrast to the known controllers. In future work, the presented controller will be investigated for stability of the closed-loop system in the disturbed case and be applied to real-world problems.

APPENDIX A

DERIVATION OF THE DISCRETE-TIME PLANT MODEL

Defining the discrete-time state $\varphi_k := \frac{1}{h} \int_{kh}^{(k+1)h} \varphi(\tau) d\tau$ and the unknown discrete-time input $\Delta_k := \frac{1}{h} (\varphi_{k+1} - \varphi_k)$ yields

$$\begin{aligned} \Delta_k &= \frac{1}{h^2} \left(\int_{(k+1)h}^{(k+2)h} \varphi(\tau) d\tau - \int_{kh}^{(k+1)h} \varphi(\tau) d\tau \right) \\ &= \frac{1}{h^2} \int_{kh}^{(k+1)h} \varphi(\tau + h) - \varphi(\tau) d\tau. \end{aligned}$$

As $|\dot{\varphi}(t)| = |\Delta(t)| \leq L \forall t > 0$, $\varphi(t+h) - \varphi(t) \leq Lh$ holds, and further $\Delta_k \in [-L, L]$. Defining $x_{1,k} := x_1(kh)$ yields the discrete-time plant model (9). Note that the plant state φ_k can be interpreted as the mean value of $\varphi(t)$ in the interval $t \in [kh, (k+1)h)$ and φ_k as well as Δ_k are virtual values.

APPENDIX B

DERIVATION OF THE LOW-CHATTERING DISCRETIZATION

The discrete-time differentiator according to [14] with a differentiation order of 1 and a filtering order of 0 is given

by

$$\begin{aligned} z_{0,k+1} &= z_{0,k} + h z_{1,k} - h \tilde{\lambda}_1 \hat{L}^{\frac{1}{2}} [z_{0,k} - f_{0,k}]^{\frac{1}{2}} \\ z_{1,k+1} &= z_{1,k} - h \tilde{\lambda}_0 \hat{L} [z_{0,k} - f_{0,k}]^0, \end{aligned} \quad (16)$$

where $f_{0,k}$ is the discrete-time signal to be differentiated, λ_1 and λ_0 are constant parameters and $z_{0,k}$ and $z_{1,k}$ are the observer states that estimate the signal $f_{0,k}$ and its first derivative $f_{1,k}$, respectively. Further, \hat{L} is an adaptive parameter following the computation law

$$\hat{L} = L \cdot \text{sat} \left(\frac{|z_{0,k} - f_{0,k}|}{L k_L h^2} \right),$$

with L being the known Lipschitz constant of the unknown signal $f_{1,k}$ and a constant parameter k_L . Selecting $\tilde{\lambda}_0 L = \beta$, $\tilde{\lambda}_1 L^{\frac{1}{2}} = \alpha$ and $L k_L = \beta$ yields the error dynamics of the differentiator (16)

$$\begin{aligned} x_{1,k+1} &= x_{1,k} + h x_{2,k} - h \alpha \text{sat} \left(\frac{|x_{1,k}|}{\beta h^2} \right)^{\frac{1}{2}} [x_{1,k}]^{\frac{1}{2}} \\ x_{2,k+1} &= x_{2,k} - h \beta \text{sat} \left(\frac{|x_{1,k}|}{\beta h^2} \right) [x_{1,k}]^0, \end{aligned} \quad (17)$$

with $x_{1,k} = z_{0,k} - f_{0,k}$ and $x_{2,k} = z_{1,k} - f_{1,k}$.

Therefore, by setting

$$\begin{aligned} u_k &= -\alpha \text{sat} \left(\frac{|x_{1,k}|}{\beta h^2} \right)^{\frac{1}{2}} [x_{1,k}]^{\frac{1}{2}} + h \beta \text{sat} \left(\frac{x_{1,k}}{\beta h^2} \right) + v_{k+1} \\ v_{k+1} &= v_k - h \beta \text{sat} \left(\frac{x_{1,k}}{\beta h^2} \right) \end{aligned}$$

the closed-loop dynamics of system (9) will follow the dynamics (17), which yields the controller functions in (8).

REFERENCES

- [1] Y. Shtessel, C. Edwards, L. Fridman, and A. Levant, *Sliding Mode Control and Observation*. Birkhauser, 2013, p. 356.
- [2] V. Acary, B. Brogliato, and Y. V. Orlov, "Chattering-free digital sliding-mode control with state observer and disturbance rejection," *IEEE Transactions on Automatic Control*, vol. 57, no. 5, pp. 1087–1101, 2012.
- [3] A. Levant, "Discretization issues of high-order sliding modes," *IFAC Proceedings Volumes*, vol. 44, no. 1, pp. 1904–1909, 2011.
- [4] V. Acary and B. Brogliato, "Implicit Euler numerical scheme and chattering-free implementation of sliding mode systems," *Systems & Control Letters*, vol. 59, no. 5, pp. 284–293, 2010.
- [5] A. Levant, "Sliding order and sliding accuracy in sliding mode control," *International Journal of Control*, vol. 58, no. 6, pp. 1247–1263, 1993.
- [6] J. A. Moreno and M. Osorio, "Strict Lyapunov Functions for the Super-Twisting Algorithm," *IEEE Transactions on Automatic Control*, vol. 57, no. 4, pp. 1035–1040, 2012.
- [7] Y. Chen, H. Dong, J. Lu, X. Sun, and L. Guo, "A Super-Twisting-Like Algorithm and Its Application to Train Operation Control With Optimal Utilization of Adhesion Force," *IEEE Transactions on Intelligent Transportation Systems*, vol. 17, no. 11, pp. 3035–3044, 2016.
- [8] A. D. Pizzo, L. P. D. Noia, and S. Meo, "Super twisting sliding mode control of smart-inverters grid-connected for PV applications," in *IEEE International Conference on Renewable Energy Research and Applications*, 2017, pp. 793–796.
- [9] B. Brogliato, A. Polyakov, and D. Efimov, "The implicit discretization of the super-twisting sliding-mode control algorithm," in *IEEE International Workshop on Variable Structure Systems*, 2018, pp. 349–353.
- [10] X. Xiong, G. Chen, Y. Lou, R. Huang, and S. Kamal, "Discrete-Time Implementation of Super-Twisting Control With Semi-Implicit Euler Method," *IEEE Transactions on Circuits and Systems II: Express Briefs*, vol. 69, no. 1, pp. 99–103, 2022.
- [11] S. Koch, M. Reichhartinger, and M. Horn, "On the Discretization of the Super-Twisting Algorithm," in *IEEE Conference on Decision and Control*, 2019, pp. 5989–5994.
- [12] B. Brogliato, A. Polyakov, and D. Efimov, "The Implicit Discretization of the Supertwisting Sliding-Mode Control Algorithm," *IEEE Transactions on Automatic Control*, vol. 65, no. 8, pp. 3707–3713, 2020.
- [13] S. Koch and M. Reichhartinger, "Discrete-time equivalents of the super-twisting algorithm," *Automatica*, vol. 107, pp. 190–199, 2019.
- [14] A. Hanan, A. Levant, and A. Jbara, "Low-chattering discretization of sliding mode control," in *IEEE Conference on Decision and Control*, 2021, pp. 6403–6408.
- [15] A. Emami-Naeini and G. Franklin, "Deadbeat control and tracking of discrete-time systems," *IEEE Transactions on Automatic Control*, vol. 27, no. 1, pp. 176–181, 1982.